Chemical Engineering Communications

ISSN: 0098-6445 (Print) 1563-5201 (Online) Journal homepage: http://www.tandfonline.com/loi/gcec20

Effect of particle size on thermal decomposition and devolatilization kinetics of melon seed shell

Awwal Ahmed, Eyitayo Amos Afolabi, Mohammed Umar Garba, Umaru Musa, Mohammed Alhassan & Kariim Ishaq

To cite this article: Awwal Ahmed, Eyitayo Amos Afolabi, Mohammed Umar Garba, Umaru Musa, Mohammed Alhassan & Kariim Ishaq (2019): Effect of particle size on thermal decomposition and devolatilization kinetics of melon seed shell, Chemical Engineering Communications, DOI: 10.1080/00986445.2018.1555530

To link to this article: https://doi.org/10.1080/00986445.2018.1555530

Published online: 14 Jan 2019.

CHEMICAL ENGINEERING COMMUNICATIONS
https://doi.org/10.1080/00986445.2018.1555530

Effect of particle size on thermal decomposition and devolatilization kinetics of melon seed shell

Awwal Ahmed, Eyitayo Amos Afolabi, Mohammed Umar Garba, Umaru Musa, Mohammed Alhassan, and Kariim Ishaq

Chemical Engineering Department, Federal University of Technology, Minna, Nigeria

ABSTRACT

Thermogravimetric analysis (TGA) and devolatilization kinetics of melon seed shell (MSS) at different particle sizes (150 μm and 500 μm) and at different heating rates (10, 15, 20, and 25 °C/min) were investigated with the aid of TGA. The results of the TGA analysis show that the TGA curves corresponding to the first and third stages for 150 μm particle sizes exhibited some bumps that developed at the first and third stages of pyrolysis. It was also observed that at constant heating rate, the maximum peak temperature increases as the particle sizes increase from 150 to 500 μm, whereas 500 μm particle sizes exhibited higher peak temperatures compared to 150 μm particle sizes. The resulting TGA data were applied to the Kissinger (K), Kissinger–Akahira–Sunose (KAS) and Flynn–Wall–Ozawa (FWO) methods and kinetic parameters (activation energy, E and frequency factor, A) were determined. The E and A obtained using K method were 74.27 kJ mol^{-1} and 3.84×10^5 min^{-1} for 150 μm particle size, whereas for 500 μm particle size were 97.12 kJ mol^{-1} and 3.74×10^7 min^{-1}, respectively. However, the average E and A obtained using KAS and FWO methods were 82.35 kJ mol^{-1}, 1.29×10^7 min^{-1}, and 88.50 kJ mol^{-1}, 1.32×10^7 min^{-1} for 150 μm particle sizes. While for 500 μm particle sizes, the E and A were 108.46 kJ mol^{-1}, 3.14×10^9 min^{-1}, and 113.05 kJ mol^{-1}, 7.56×10^9 min^{-1}, respectively. It was observed that E and A calculated from FWO and KAS methods were very close and higher than that obtained by K method. It was observed that the minimum heat required for the cracking of MSS particles into products is reached later at higher peak temperatures since the heat transfer is less effective as they are at lower peak temperatures.

KEYWORDS

Activation energy; Biofuel; Decomposition; Kinetics; Melon seed shell; Pyrolysis

Introduction

Fossil fuels are the most dominant source of global energy supply. Reports have shown that present world petroleum reserves would suffice for some few more decades (Garba, 2013; Musa et al., 2014a). In addition to this depletion, the continuous use of fossil-derived fuels is the major contributor to global warming. The increasing concerns for these greenhouse gas emissions, soaring price of petroleum-derived fuel, and uncertainty about its continuous supply in Nigeria have led to the recent ongoing search for renewable alternative energy sources (Garba et al., 2006, 2014, 2017a; Musa et al., 2014b, 2015). Renewable energy sources are presently the most globally accepted alternative source of energy due to their low carbon impact and guarantee of sustainable feedstock supply. Renewable energy accounts for about 13% of global energy supply and 1.3% of these sustainable energy come from biomass (Ho et al., 2014).

Biomass is currently the most important renewable energy feedstock and ranks as the fourth largest source of energy in the world, after coal, oil, and natural gas. According to Garba et al. (2017a), approximately 144 million tons of biomass resource are generated annually in Nigeria. These large quantities of agricultural residues have the capacity for meeting and diversifying the nation energy supply (John, 2011). These will eventually lead to rural economic development, market diversification, boosting the nation's international competitive strength and leads to appreciable decline in environmental

CONTACT Mohammed Umar Garba umar.garba@futminna.edu.ng Federal University of Technology, Minna, Niger State, P. M. B. 65, Nigeria.
Color versions of one or more of the figures in the article can be found online at www.tandfonline.com/gcec.

pollution (Jekayinfa and Omisakin, 2005). In recent time, the Energy Commission of Nigeria stated that its long-term (2016–2025) plan on the nation's energy requirements is completely non-fossil (Musa and Aberuagba, 2012). The commission intends to generate about 36% of the nation's electricity need from renewable energy resources in which biomass is a significant part. Biomass conversion into energy resources can be carried out via two main conversion routes namely, thermochemical and biochemical routes.

Thermochemical conversion routes include combustion, gasification, pyrolysis, cofiring, and liquefaction. All these processes result into breakage of bonds between the adjacent carbon, hydrogen, and oxygen molecules to release the stored and chemical energy. Pyrolysis (devolatilization) as a thermochemical conversion process is one of the first steps of combustion, gasification, and liquefaction processes (Nithitorn et al., 2015; Garba et al., 2017b). The yields of liquids, char, and gases obtained from biomass pyrolysis process are dependent on the feedstock type, particle size, heating rate, temperature, and residence time The size and the mass of particles are some of the most important parameters that is profoundly influenced by the heat and mass transfer limitations. The larger the particle size, the more effective the heat transfer causing the release of more volatiles. Several studies reported the effect of different particle sizes of various biomass materials on char, liquid, and gas yield (Demirbas 2004; Mani et al., 2010).

The explicit understanding of the thermal behaviors and combustion kinetics of biomass is a prerequisite for modeling industrial combustion behaviors in furnaces either using biomass or biomass-coal blends (Munir et al. 2009). Kinetics data are also vital for the design and development of a highly efficient biomass thermochemical conversion processing systems (Cai et al., 2008; Shen et al., 2009).

Different kinetic models have been well established for the evaluation of non-isothermal solid state kinetic studies using thermogravimetric analysis (TGA) data. These methods are usually classified into model-free and model-fitting methods (Kissinger, 1956; Ozawa, 1965; Flynn & Wall 1966; Alberto, 2008; Sachin et al., 2011; Fantozzi et al., 2016; Bartocci et al., 2017). For applying the model-free model, knowledge of the reaction mechanism is not required for the evaluation of kinetic parameters, whereas the model-fitting method employs a mass-dependent function for kinetic parameters evaluation. Interestingly, model-fitting methods could be subdivided into single component or multiple components depending upon whether the biomass is characterized (wholly as a unit or based on its lignocellulose components) and by the products definition. This can either be a lumped products of gas, char, and tar or individual species present in the lump products. Typical examples of model-free method include Kissinger (K), Kissinger–Akahira–Sunose (KAS) and Flynn–Wall–Ozawa (FWO) methods. The obvious distinction between K and the other isoconversional methods (KAS and FWO) is that while the former accounts only for the actual kinetic parameters values, the latter evaluates the apparent values of kinetic parameters as a summation of the physical process and chemical transformation occuring in the pyrolysis process. The thermal degradation and kinetics analysis of a number of biomass materials using these models have been documented in literatures (Alberto, 2008; Katarzyna et al., 2012; Vanita et al., 2011; Niu et al., 2013; Bhavanam and Sastry, 2015; Fantozzi et al., 2016; Bartocci et al., 2017). Slopiecka et al. (2012) reported the thermal degradation of poplar wood using the three methods (K, FWO, and KAS). The study evaluated the kinetic of this biomass decomposition. The results revealed that better accuracy was obtained from KAS and FWO methods. Abdelouahed et al. (2017) investigated the comparative reliability of K, KAS, Friedman, and least square minimization methods on the thermal decomposition of flax shives and beechwood and their respective lignocellulose components. The authors reported that Kissinger method demonstrated appreciable reliability in comparison with other methods for determination of kinetic parameters of the pure components. While for biomass materials, least square minimization method was reported to be more appropriate for the kinetic data deduction. More recently, Bartocci et al. (2017) proposed a novel reaction scheme for biomass components

and glycerol using the model-fitting methods. Findings from this study revealed that the reaction was satisfactorily described by first reaction order with the exception for the recalcitrant lignin whose degradation fitted well to a second reaction order. Nearly in all of these studies, varying thermal behavior and kinetic data were deduced. According to Braz and Crnkovic (2014), the variation in biomass thermal behaviors is primarily due to its natural diversity and possession of unique properties. The authors further added that the thermal behaviors in addition to biomass heating values, proximate composition, and ultimate composition were obvious indicators of biomass fuel quality.

For better understanding of thermal degradation of biomass, many researchers had studied thermal decomposition of biomass by TGA. This biomass includes corn stover, coconut and cashew nut shell (Alberto, 2008), wood chips (Lukas et al., 2009), oil palm shell, rice husk (RH), oil palm frond, and paddy straw, groundnut cake (Sachin et al., 2011), baggase (Vanita et al., 2011), poplar wood (Katarzyna et al., 2012), coffee husk, tucuma seed, sugar cane baggase, peanut shell, RH, and pine sawdust (Braz and Crnkovic, 2014), and de-oiled seeds cake of African star apple (Sokoto et al., 2016).

Melon seed (*Citrullus colocynthis L.*) belongs to the genus *Citrullus* of cucurbitaceae family. *Citrullus colocynthis L.* is one of the 300 species of melon found in tropical Africa. The seed contains about 53% of oil and 28% of protein. Melon is known to be also cultivated in Middle East region of the world and most part of Africa as food. In Nigeria, it is cultivated over an estimated land area of about 361,000 ha with a corresponding seed production capacity of 347,000 tons as at 2002. It is mainly used for preparation of local soup in Nigerian. Melon kernels are usually enclosed in a shell which has to be removed during its processing food application (Bande et al., 2012). It has been reported that large amount of these shells are usually thrown away and burnt in open air, thereby resulting into environmental pollution (Ogbe and George, 2012). Nyakuma (2016) reported that the use of melon shell for eco-friendly bioenergy synthesis and other green value-added products is yet to be explicitly exploited. This is due to the lack of adequate understanding of the thermochemical fuel properties and behavior of this waste material. The author added that melon shell is a viable renewable raw material for the production of solid, liquid, and gaseous biofuels via thermochemical conversion routes.

Reviewing of the open literature suggests that biomass type and process parameters (heating rate, temperature, and particle size) have impact on their thermal and kinetic behavior. Despite a number of remarkable studies in the literature, there still remains a lot of information on the particle size that is not recognized in sufficient detail. Most reported studies show the effect of particle size on pyrolysis product yield (Demirbas, 2004; Mani et al., 2010). In this work, a comparative evaluation of different particle size of MSS has been studied to gain overall understanding of the thermal and kinetic behavior. In this regard, the thermal events occurring during pyrolysis of biomass with different particle sizes were identified with the view of generating kinetic data that can be effectively used for design and optimization of thermochemical processing system.

Materials and methods

Sample preparation

Biomass sample used for the experiment is MSS sourced from Paiko town, Paikoro Local Government of Niger State, Nigeria. MSS sample was dried in an oven at a temperature of 105 °C for 3 h for moisture content removal and to aid grinding. The sample was then crushed using mortar and pestle for particle size reduction. Subsequently, the reduced particle sizes were ground with blender and sieved via 150 and 500 sieves. The particles that passed through the two sieves openings were collected and stored in sample bottles for further analysis.

Characterization

Proximate analysis was carried out by subjecting 200 mg of ground MSS sample at temperature between the room temperature to 600 °C, for moisture content (MC), ash content (AC), and volatile content (VC) determination according to E871, D1102, and E872 standard ASTM technique, respectively. Fixed carbon content (FC)

was determined by subtracting sum of MC, AC, and VC from 100 percent. Ultimate analysis was carried out using carbon, hydrogen, nitrogen, and sulfur (CHNS) elemental analyzer. The details can be found in Lukas et al. (2009).

Pyrolysis of MSS was performed using Perkin Elmer thermogravimetric analyser (TGA-4000). The analyzer was first purged with nitrogen gas at flow rate of 20 ml/min and pressure of 2.5 bars to create an inert environment. Approximately 25 ± 2 mg of MSS was loaded into empty crucible inside the analyzer. Then, the heating rate was controlled at 10, 15, 20, or 25 °C/min and temperature ranges from 25 to 625 °C. The above procedure was repeated for two different particle sizes of 150 and 500 µm. The data generated by the TGA machine were processed using the Pyris Manager software by Perkin Elmer Corporation.

Kinetic theory

Biomass pyrolysis takes place in the presence of nitrogen or other inert gas to produce solid char and volatile matter. The overall conversion can be represented by Equation (1), using one-step global model (Basu, 2010).

$$Biomass \xrightarrow{k(T)} Solid\ (Char)\ +\ Volatile \tag{1}$$

while the kinetics of reaction of the biomass pyrolysis in Equation (1) can be represented by Equation (2).

$$\frac{d\alpha}{dt} = k(T)f(\alpha) \tag{2}$$

Where $\frac{d\alpha}{dt}$ is the conversion rate of biomass at constant temperature, $k(T)$ is the reaction rate constant, $f(\alpha)$ is the differential model of the reaction, and α is the conversion or extent of reaction, the normalized form of weight data of decomposed sample, is expressed as follows:

For isothermal TGA

$$\alpha = \frac{W_i - W_t}{W_i - W_f} \tag{3}$$

Where w_i, w_f, and w_t are the initial weight of the sample, final weight after decomposition, and sample weight at time, t respectively.

For non-isothermal TGA

$$\alpha = \frac{W_i - W_t}{W_i - W_f} \tag{4}$$

Where w_t is the sample weight at temperature, T.

Also according to Arrhenius equation, the temperature-dependent rate constant is represented below:

$$k(T) = Ae^{-\frac{E}{RT}} \tag{5}$$

Where A is the frequency factor (min^{-1}), E is the activation energy ($kJmol^{-1}$), T is the absolute temperature in Kelvin, and R is the gas constant (8.314 JK^{-1} mol^{-1}).

Substituting Equation (5) into Equation (2) gives Equation (6), which is fundamental equation that can be used to determine kinetic parameters using analytical methods, on the basis of TGA results.

$$\frac{d\alpha}{dt} = Ae^{-\frac{E}{RT}}f(\alpha) = Af(\alpha)e^{-\frac{E}{RT}} \tag{6}$$

Where

$$f(\alpha) = (1-\ \alpha)^n \tag{7}$$

And n is the order of reaction. Substituting Equation (7) into Equation (6) gives:

$$\frac{d\alpha}{dt} = A(1-\alpha)^n e^{-\frac{E}{RT}} \tag{8}$$

and for non-isothermal TGA experiments at linear heating rate:

$$T = T_0 + \beta t \tag{9}$$

where T_0 is the starting temperature, β is the constant heating rate, and T is the temperature at time t.

Therefore, the differential of temperature with respect to time:

$$\frac{dT}{dt} = \beta \quad \text{Consequently } dt = \frac{dT}{\beta} \tag{10}$$

Substituting Equation (10) into Equation (8) gives:

$$\frac{d\alpha}{dT} = \frac{A}{\beta}(1-\ \alpha)^n e^{-\frac{E}{RT}} \tag{11}$$

where $\frac{d\alpha}{dT}$ is the conversion rate of biomass at constant time. Equation (11) can be used for non-isothermal TGA to calculate kinetic

Table 1. Physical analysis of MSS and other solid fuels.

Proximate	MSS	RH*	GNS*	Coal°
MC (wt. %)	3.52	3.81	8.44	
VC (wt. %)	80.14	66	63.81	
AC (wt. %)	2.12	8.18	8.42	
FC (wt. %)	14.22	22.01	19.33	
Ultimate analysis				
C	52.01	43.83	45.32	74.12
H	6.50	6.76	6.03	4.22
O	39.60	46.07	43.54	6.93
N	1.65	0.93	0.51	1.91
S	0.24			

*Garba et al. (2017a); °Wang et al. (2001).

parameters and for the purposes of this study, kinetics of MSS was evaluated using non-isothermal model-free methods, namely, K, KAS, and FWO methods, respectively.

Model-free methods

Because of several problems associated with model-fitting methods such as inability to uniquely determine the reaction model, this has led to the decline in usage of these methods over model-free methods which are isoconversional. Although model-free methods are isoconversional with exception of Kissinger method which does not calculate activation energy at progressive value of conversion, but assumed a constant value (Katarzyna et al., 2012). Model-free methods evaluate kinetics of biomass pyrolysis without modelistic assumption.

The K method is based on Equation (12) and it involves plotting the terms $\ln(\beta/T_m{}^2)$ against $1/T_m \times 10^{-3}$, where T_m is the peak temperature obtained from DTG curve.

$$\ln\left\{\frac{\beta}{T^2{}_m}\right\} = \ln\left\{\frac{AR}{E}\right\} - \frac{E}{RT_m} \tag{12}$$

where E, activation energy can be calculated from the slope $-E/R$ and A, frequency factor from the intercept $\ln(AR/E)$ of the linear graph.

The KAS method is based on Equation (13) and it involves plotting the terms $\ln(\beta/T^2{}_\alpha)$ against $1/T_\alpha \times 10^{-3}$ (Kissinger, 1956)

$$\ln\left\{\frac{\beta_i}{T^2{}_{\alpha i}}\right\} = \ln\left\{\frac{A_\alpha R}{E_\alpha g(\alpha)}\right\} - \frac{E_\alpha}{RT_{\alpha i}} \tag{13}$$

where E_α, apparent activation energies can be calculated from the slope $(-E_\alpha/R)$ and A_α, frequency factors from the intercept $(\ln\{A_\alpha R/E_\alpha g(\alpha)\})$ of the linear graphs. Integral model of the reaction, $g(\alpha)$ is constant at a known value of conversion.

The FWO method is based on Equation (14) and its involves plotting the terms $\ln(\beta)$ against $1/T_\alpha \times 10^{-3}$ (Ozawa, 1965; Flynn & Wall 1966).

$$\ln\beta = \ln\left\{\frac{A_\alpha E_\alpha}{Rg(\alpha)}\right\} - 5.331 - 1.052\frac{E_\alpha}{RT_\alpha} \tag{14}$$

where E_α, apparent activation energies can be calculated from the slope $(-E_\alpha/R)$ and A_α, frequency factors from the intercept $(\ln\{A_\alpha E_\alpha/Rg(\alpha)\} - 5.331)$ of the linear graphs.

Results and discussion

The basic properties of the MSS such as proximate, fiber, and ultimate analyses are given in Table 1. To provide insight into the thermal behavior, the samples were crushed and sieve into particle sizes of 150 and 500 µm sieves used.

Physiochemical properties

Proximate analysis is the easiest and fastest way of evaluating fuel characteristics of solid biomass (Sachin et al., 2011). Table 1 compares the proximate and ultimate analyses of MSS from this study to RH, ground nut shell (GNS), and coal from the literature. From Table 1, it was shown that MSS has low MC and AC of 3.52 wt.% and 2.12 wt.%, respectively, which make it suitable for combustion and other thermochemical conversion processes (McKendry, 2002). High content of ash is not desirable because it influences slag formation and composition on the wall of combustion furnaces and boilers (Sachin et al., 2011, Garba et al., 2016). Also, Table 1 shows that MSS has high VC of 80.14wt. %. This high VC is a measure of its ease of ignition and an indication that the loss in FC during devolatilization is minute. The high VC also signifies higher tendency of MSS conversion to liquid or gaseous fuels in comparison to solid fuels production (Sachin et al., 2011; Garba et al., 2012). VC to FC ratio of 5.64 obtained is within the stipulated range of greater than 4 reported for a typical biomass.

The result of ultimate analysis of the MSS revealed high percentage of C (52.01%) and O

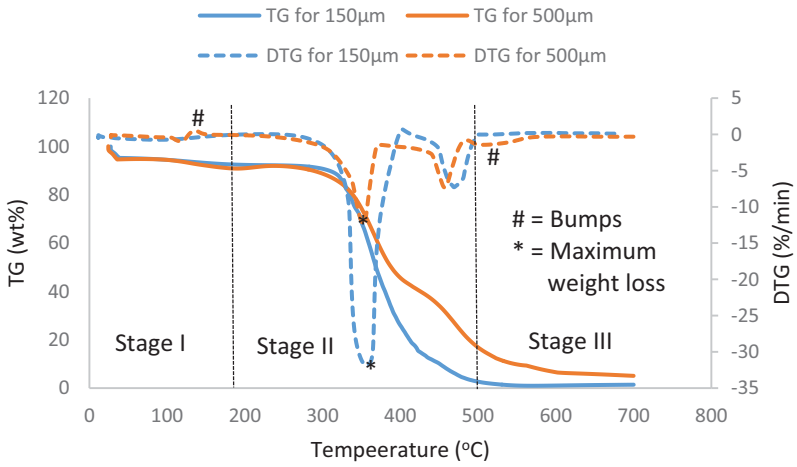

Figure 1. TG and DTG curves for 150 and 500 µm particle sizes.

(39.60%) when compared with H, N, and S with relatively lower composition. It was noticed that the combined percentage composition of carbon and hydrogen is higher than that of O and N. It also indicates that sulfur has the lowest percent composition. Low nitrogen and sulfur content make MSS more environmental friendly for use in production of clean energy.

Effect of particle size on thermal decomposition

TGA offers essential thermographs that can be used to interpret the thermal behavior of solid fuel (Ounas et al., 2011). Such thermographs clarify the complications involved in the thermal decomposition of the solid fuel. Thus, the pyrolysis kinetics deduced from the thermographs are used in the design and control of pyrolysis reactor (Zhou et al., 2013; Garba et al., 2018).

TGAs of MSS for two different particle sizes (150 and 500 µm) are displayed in Figure 1. In this figure, the differential weight loss at four different heating rates (10, 15, 20, and 25 °C/min) are shown. As expected, a typical differential weight loss at three different regions were observed which correspond to water removal, main devolatilization, and continuous slight devolatilization (Munir et al., 2009; Slopiecka et al., 2012). Figure 2(a,b) depicts the devolatilization process which starts at about 185 °C and proceeds with a significant drops in weight until about 494 °C and then the weight drop gradually to the final temperature. The first stage (drying stage) of the decomposition which begins from room temperature to 180 °C is associated with moisture removal, mainly associated with evaporation of water content. The second stage (main devolatilization) covered the regions of maximum weight loss (*) corresponding to the characteristic peak temperatures at the range of 180 °C–481 °C. According to Nithitorn et al. (2015) and Sokoto et al. (2016), this stage is associated with removal of hemicellulose and cellulose, respectively. While the third stage which covered a wider temperature range of 481 °C–625 °C is associated with lignin removal (Slopiecka et al., 2012).

Figure 1 shows that the curves of TG and DTG profiles at a heating rate of 10 °C/min shift toward higher temperatures as the particle size increased from 150 to 500 µm. The effect of particle size on mass transfer can be explained by two opposite aspects: the first one is that the larger the particle size is, the smaller the heat transfer resistance which improves heat and mass transfer and therefore has faster decomposition process. In this way, lighter volatile is released and less char is produced at the final temperature (Slopiecka et al., 2012). From Figure 1, a negligible char yields of about 0.077% was produced from the thermal degradation of MSS of particle size of 500 µm. In the second aspect, the smaller particle size causes a delay in the resident time of volatile matter released due to larger surface area. The presence of large surface area exhibited by this particles results into slower decomposition process and the production of more char at the final temperature. It can be observed from Figure

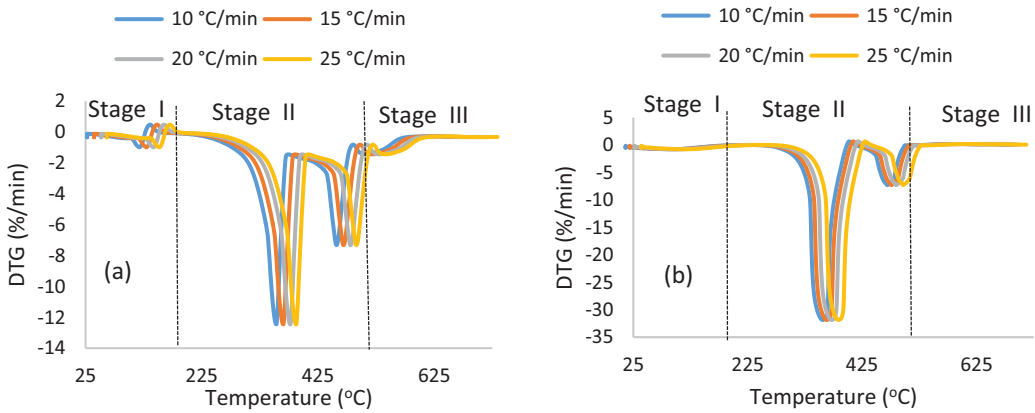

Figure 2. DTG curves at different heating rates for (a) 150 µm and (b) 500 µm particle sizes.

3 that the residual char yield of about 5.074% was produced in the course of thermal degradation of MSS of a particle sizes of 150 µm as against 0.077% for a particle size of 500 µm. It is very evident from the results that increasing particle size resulted in a decrease in the values of the residual char yield. This result is in agreement with the results of Slopiecka et al. (2012).

For the two different particle sizes (150 and 500 µm) studied, the pyrolysis pattern was similar in all the stages except for some bumps (#) that developed at the first and third stages of pyrolysis for 150 µm particle sizes (Figure 1). A close observation of the DTG curves in Figure 1 shows that a bump developed (inconsistent weight loss) at a peak temperature of 119 °C for 150 µm particle sizes. The observed structure can be attributed to the buoyancy effect introduced by the nitrogen flow into the TGA system during the analysis process. It is significant to point out that as the devolatilization process approaches the final degradation temperature, the smaller particle sizes (150 µm) char developed another bump due to prolong heating. This observation shows appreciable consistency with a report of Chen et al. It is noteworthy that the small bump that appears in 150 µm particle size was not visible on the curve for 500 µm particle sizes. This revealed that MSS with a larger particle size induced an improved effective heat transfer which will, in turn, lead to the complete decomposition of lignin resulting into the bump disappearance.

The effect of heating rates on pyrolysis product yields and characteristics are essential for the design of efficient pyrolysis reactor. The characteristics of the products are expressed by TGA in terms of change in weight as a function of temperature. The differential weight loss significantly amplifies the changes in weight during main devolatilization process. However, as the heating proceeds, the solid residue undergo further devolatilization process to a final temperature.

From Figure 2(a,b), it can be observed that the maximum rate of derivative weight loss (minimum points of DTG curves) occurs at the peak temperatures. The corresponding peak temperatures of 150 µm particle sizes were 353.1 °C, 365.1 °C, 377.21 °C, and 387.22 °C for 10, 20, 30, and 40 °C/min heating rate, respectively, as shown in Figure 2(a). While for particle size of 500 µm, the peak temperatures corresponding (let this be removed) were 468.96 °C, 476.13 °C, 484.59 °C, and 496.65 °C for 10, 20, 30, and 40 °C/min heating rate, respectively, in Figure 2(b). The peak temperatures of 500 µm particle sizes are larger than that of 150 µm particle size by the difference of 115.86 °C, 111.03 °C, 107.38 °C, and 109.43 °C for 10, 20, 30, and 40 °C/min heating rate, respectively. The whole differential weight loss shifted toward a higher temperature regions with increased heating rates and larger particle sizes exhibited higher peak temperatures compared to smaller particle sizes. The shift in weight loss toward higher temperature was in agreement with study of Slopiecka et al. (2012) during the investigation of the effects of the non-isothermal pyrolysis of poplar wood. This observation was also in agreement with findings of Senneca (2007), Katarzyna et al. (2012), Mahir

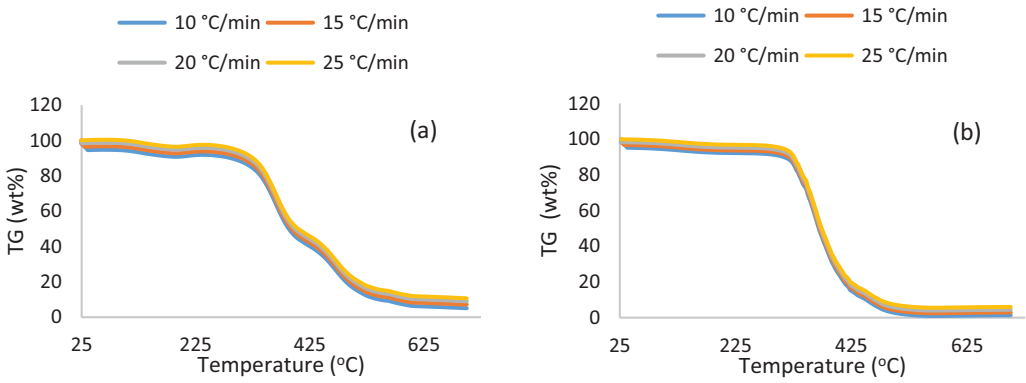

Figure 3. TG curves at different heating rates for (a) 150 µm and (b) 500 µm particle sizes.

et al. (2014), Nithitorn et al. (2015), and Sokoto et al. (2016), respectively.

The TG curve in Figure 3 shows weight loss versus temperature at different heating rates for MSS. As can be observed from the figure, the devolatilization process begins at about 185 °C and the weight loss declines steeply with increasing temperature until the temperature reached about 494 °C and then the weight loss declines gradually to the final temperature. The dehydration region does not change because the heating rate used for drying was same for each TGA (Figure 3).

The solid residue yields are about 5.074% and 0.077% for particle sizes of 150 and 500 µm, respectively. The solid residue yields obtained from the final temperature for 150 µm particle sizes (5.074%) is higher compared to that of 500 µm particle sizes (0.077%), which also translate to longer residence time (Idris et al., 2012).

Devolatilization kinetics

The main goal of kinetic study of biomass pyrolysis is to determine the activation energy, which is the measure of ease of occurrence of reaction. Reaction process with lower activation energy takes place more easily than the one with higher activation energy (Sachin et al., 2011). For the purpose of this study, activation energy and frequency factor also known as kinetic parameters were determined using model-free methods, namely, K, KAS, and FWO methods.

The kinetic parameters E, A, and R from Equations (12), (13), and (14) correspond to K, KAS, and FWO methods, respectively. This method involves the calculation of kinetic parameters E, A, and R from the heating rates of 5, 10, and 20 °C/min and their peak decomposition temperatures, respectively. Subsequently, E and A were extracted from the slope and intercept of plot regression line in Figure 1. K, KAS, and FWO plots of ln (β/T_m^2) versus 1000/T (K^{-1}) for 150 and 500 µm particle sizes are shown in Figures 4–6, respectively. However, for KAS and FWO, the plots of ln $(\beta i/T_{\alpha i}^2)$ versus $1000/T_{\alpha i})$ K^{-1} for different degree of conversions are shown in Figure 7. High value of R^2 (greater 0.9) shows good fitting to straight lines suggesting that first-order reaction model suffices. For K method at 150 µm, the values of 74.27 kJ mol^{-1}, 3.84 × 10^5 min^{-1}, and 0.9775 were obtained for E, A, and R^2, respectively. While at 500 µm, the values of 97.12 kJ mol^{-1}, 3.74 × 10^7 min^{-1}, and 0.9339 were obtained for E, A, and R^2, respectively. The K method has been reported in open literature to determine the kinetic parameters of biomass material.

The value of conversion 0.1 to 0.8 was chosen because at conversion rates less than 0.1 or above 0.8 have low correlation values, and therefore excluded (Ceylan and Topcu, 2014). Figures 4–6 show that most of fitted lines are nearly parallel to each other, indicating similar decomposition mechanisms, whereas for those lines that are not parallel to one another probably multiple/complex mechanisms is occurring (Vanita et al., 2011). The values of E for the fuel at 150 µm were observed to increase from 59.77 kJ/mol (α = 0.10) to 74.27 kJ/mol (α = 0.30), then remain constant 74.27 kJ/mol (α = 0.4) before increasing to 114.32 kJ/mol (α = 0.80) which results in the

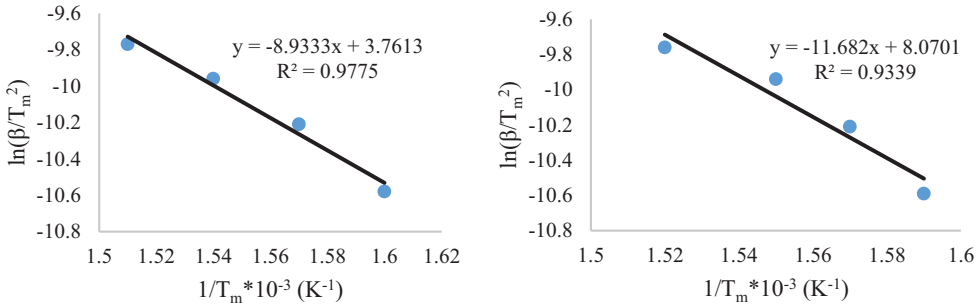

Figure 4. Plot for determination of kinetic parameters using Kissinger method, for 150 μm and 500 μm particle sizes.

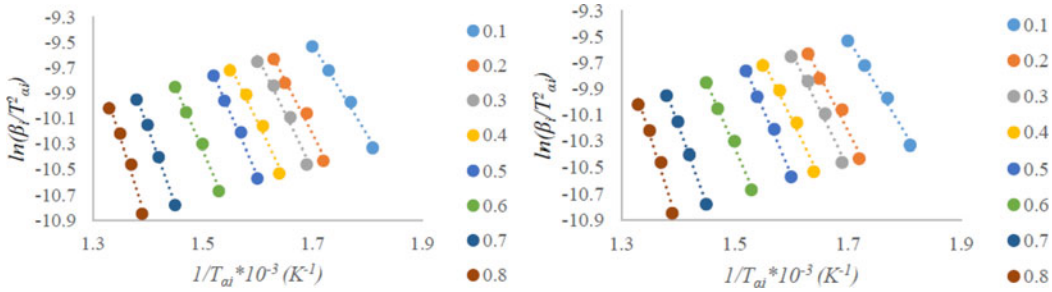

Figure 5. Plot for determination of kinetic parameters using KAS method for 150 μm and 500 μm particle sizes.

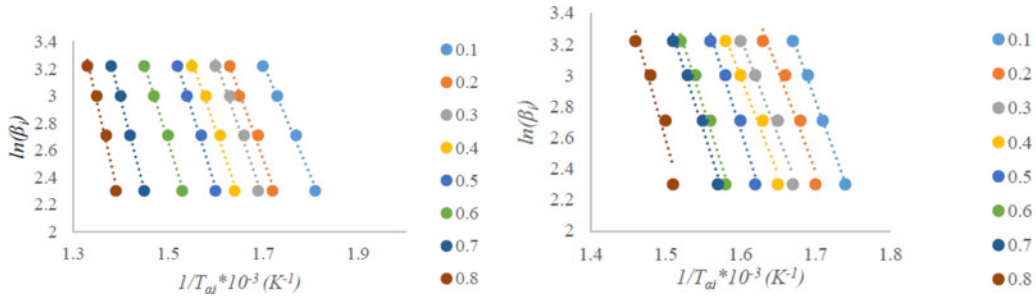

Figure 6. Plot for determination of kinetic parameters using FWO method for 150 μm and 500 μm particle sizes.

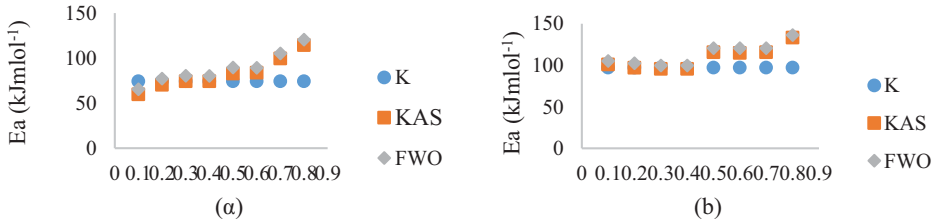

Figure 7. Effect of activation energy at a particle sizes of (a) 150 μm and (b) 500 μm.

highest activation observed during the biomass pyrolysis of MSS. For 500 μm, the values of *E* were observed to decrease from 100.86 kJ/mol (α = 0.10) to 95.47 kJ/mol (α = 0.40) and then increased to 115.56 kJ/mol (α = 0.5) before slightly decreasing to 115.56 kJ/mol (α = 0.7) and then increasing to 133.17 kJ/mol which results in the highest activation observed during the thermal analysis of MSS. Overall, the average value of activation energy for the devolatilization process at a particle size of 500 μm (108.46 kJ/mol) was higher than that of 150 μm (82.35 kJ/mol). The reason for higher activation energy during decomposition of large particle size can be explained on the basis of peak temperature. From the result in Figure 1, the pointed wider curve around the peak temperature (468.96 °C) for a particle size of 500 μm (connote higher peak temperature) than (353.1 °C) observed for a particle size of 150 μm. It was observed that the

Table 2. Values of E, A, and R^2 using K, KAS, and FWO methods for 150 μm particle size.

150 μm	KAS method			FWO method		
A	E (kJ mol^{-1})	A (min^{-1})	R^2	E (kJ mol^{-1})	A (min^{-1})	R^2
0.1	59.77	1.14×10^5	0.9912	65.38	9.07×10^4	0.9921
0.2	70.35	1.22×10^5	0.9780	77.29	1.04×10^6	0.9831
0.3	74.27	3.45×10^5	0.9775	80.35	2.32×10^6	0.9807
0.4	74.27	2.95×10^5	0.9775	80.35	1.99×10^5	0.9807
0.5	82.69	1.47×10^6	0.9940	89.52	1.01×10^7	0.9941
0.6	83.65	1.06×10^6	0.9929	89.52	6.05×10^6	0.9941
0.7	99.46	1.03×10^7	0.9974	105.10	4.69×10^7	0.9976
0.8	114.32	8.96×10^7	0.9809	120.52	3.87×10^7	0.9807
Average	82.35	1.29×10^7	0.9862	88.50	1.32×10^7	0.9879
K method	$E = 74.27$ kJ mol^{-1}		$A = 3.84 \times 10^5$ min^{-1}		$R^2 = 0.9775$	

Table 3. Values of E, A, and R^2 using K, KAS and FWO methods for 500 μm particle size.

500 μm	KAS method			FWO method		
A	E (kJ mol^{-1})	A (min^{-1})	R^2	E (kJ mol^{-1})	A (min^{-1})	R^2
0.1	100.86	5.71×10^7	0.9973	105.10	1.94×10^8	0.9976
0.2	96.89	3.29×10^7	0.9381	102.30	1.47×10^8	0.9450
0.3	95.47	2.58×10^7	0.9688	99.60	9.07×10^7	0.9713
0.4	95.47	2.85×10^7	0.9688	99.60	1.01×10^7	0.9713
0.5	115.56	1.59×10^9	0.9790	120.52	5.55×10^9	0.9807
0.6	114.73	9.82×10^8	0.9791	120.52	3.99×10^9	0.9807
0.7	115.56	1.30×10^9	0.9790	120.52	4.50×10^9	0.9807
0.8	133.17	2.11×10^{10}	0.9281	136.22	4.59×10^{10}	09241
Average	108.46	3.14×10^9	0.9673	113.05	7.56×10^9	0.9689
K method	$E = 97.12$ kJ mol^{-1}		$A = 3.74 \times 10^7$ min^{-1}		$R^2 = 0.9339$	

minimum heat required for the cracking of MSS particles into products is reached later at higher peak temperatures since the heat transfer is less effective as they are at lower peak temperatures. According to Haykiri-Acma (2003), high peak temperature means good reactivity of biomass sample which invariably implies higher activation energy. Similarly, Altun et al. (2003) have also reported that at high peak temperature the minimum heat required for the cracking of biomass particles into products is reached later due to ineffective heat transfer.

The values of the kinetic parameters are shown in Table 2 andTable 3 for K, KAS, and FWO methods. Comparing the three methods shows that the activation energies for KAS method (82.35 kJ mol^{-1}) and FWO method (88.50 kJ mol^{-1}) were higher than the activation energy for K method (74.27 kJ mol^{-1}). This is due to the fact that the K method accounts for only the T_{max} of the MSS, whereas KAS and FWO methods account for wider temperature range on the basis of different degree of conversions (isoconversional). According to Abdelouahed et al. (2017), the application of K method for evaluation of the kinetics of heterogenous compounds such as biomass could result into erroneous deductions. Generally, the activation energy values of MSS were within the range of the values reported for biomass materials by Sun et al. (2012). It was noticed that the average activation energy value increases as the particle sizes increase from 150 to 500 μm for all the three methods, that is from 74.27 (K method), 82.35 (KAS method), and 88.50 kJ mol^{-1} (FWO method) to 96.74 (K method), 108.46 (KAS method), and 113.05 kJ mol^{-1} (FWO method), which is in conformity with the study of Niu et al. (2013). The activation energy obtained in this study is significantly lower than the activation energy of 296 kJ/mol and 161.26 kJ/mol

Table 4. Energy of activation of biomasses calculated by other authors.

Authors	Biomass	E (kJ mol^{-1})
Nassar et al. (1996)	Bagasse	88
Zhang et al. (2006)	Wheat straw	70.516
	Wood chip	85.393
	Peanut shell	84.470
Li et al. (2008)	Corn stalks	66.518
	Cotton stalk	71.055
	poplar wood	
Zhang et al. (2016)	Douglas fir sawdust	71.70
Garba et al. (2017b)	Iroko wood	24.59
Islam et al. (2016)	Karanj fruit hulls	70.489

reported for FWO and KAS method, respectively, during thermal decomposition of melon shell husk by Nyakuma (2016). The discrepancies observed can be attributed to difference in melon varieties, climatic conditions, and storage stability. The frequency factors calculated from KAS (3.14×10^9 min^{-1}) and FWO (113.05 min^{-1}) methods were higher than the value (3.74×10^7 min^{-1}) calculated from K method. From the trend of the results, it can be deduced that conversion increases as the frequency factors increases which, in turn, led to an increase in activation energy. The *E* values obtained vary with the particle size, method, and approach used. However, the value obtained in this study is close agreement with literature data as shown in Table 4.

The effect of activation on particle sizes is shown in Figure 7. Considering KAS and FWO methods (isoconversional), for a particle sizes of 150 μm. Lower activation energy of 59.77 and 65.38 kJ mol^{-1} was initially observed after which the value begins to increase with corresponding increase in conversion up to an activation energy of 114.32 and 120.52 kJ mol^{-1}. However, for a particle size of 500 μm, higher activation energy of 100.86 and 105.10 kJ mol^{-1} were initially deduced which decreases with increase in conversion until a value of 95.47 and 99.60 kJ mol^{-1} was obtained at a conversion of 0.4 and then it remains approximately constant at 0.5–0.7 and finally it increases at 0.8 to 133.17 and 136.22 kJ mol^{-1}, respectively. From the above characteristics, it can be noticed that MSS with 150 μm particle sizes will required lower energy input as fuel in a devolatilization process than 500 μm particle sizes. This is because MSS with particle sizes of 150 μm starts at lower activation energy (KAS and FWO methods) than 500 μm, and it increases with increases in conversion. Additionally, because 150 μm particle sizes have lower average activation energy values by isoconversional method than 500 μm particle sizes. Lower activation energy of 150 μm particle sizes at the beginning of the devolatilization process than 500 μm particle sizes indicates the ease of ignition of former over the latter that begins at much higher value.

Conclusion

MSS have been analyzed with the aid of TGA to study the effects of particle size on thermal behavior and devolatilization kinetics. The resulting TGA data were applied to the K, KAS, and FWO methods and kinetic parameters (*E* and *A*) were determined. It was observed that *E* and *A* calculated obtained from FWO and KAS methods were higher than that obtained by K method due to fact that K method only accounts for maximum peak temperature. Kinetic plots of activation energy against conversion for both FWO and KAS method show that the higher the particle size, the greater the peak temperature and activation energy.

Disclosure statement

No potential conflict of interest was reported by the authors.

References

Abdelouahed, L., Leveneur, S., Vernieres-Hassimi, L., Balland, L., and Taouk, B. (2017). Comparative investigation for the determination of kinetic parameters for biomass pyrolysis by thermogravimetric analysis, *J. Therm. Anal. Calorim.*, **129**, 1201–1213. DOI: 10.1007/s10973-017-6212-9

Altun, N. E., Hicyilmaz, C., and Kök, M. V. (2003). Effect of particle size and heating rate on the pyrolysis of silopi asphaltite, *J. Anal. Appl. Pyrolysis.*, **67**, 369–379.

Bande, Y. N., Adam, N. M., Jamarei, B. O., and Azmi, Y. (2012). Physical and mechanical properties of "Egusi" Melon *(Citrullus colocynthis lanatus* var. *lanatus)* fruit, *Int. J. Agri. Res.*, **7**, 494–499.

Bartocci, P., Anca-Couce, A., Slopiecka, K., Nefkens, S., Evic, N., Retschitzegger, S., Barbanera, M., Buratti, C., Cotana, F., Bidini, G., and Fantozzi, F. (2017). Pyrolysis of pellets made with biomass and glycerol: Kinetic analysis and evolved gas analysis, *Biomass Bioenergy*, **97**, 11–19.

Braz, C. E. M., and Crnkovic, Paula C. G. M. (2014). Physical-chemical characterization of biomass samples for application in pyrolysis process, *Chemical Engineering Transactions*, **37**, 523–528. http://hdl.handle.net/11449/123598

Basu, P. (2010). *Biomass Gasification and Pyrolysis: Practical Design and Theory*. Academic press, Burlington.

Cai, J., Wang, Y., Zhou, L., and Huang, Q. (2008). Thermogravimetric analysis and kinetics of coal/plastic blends during co-pyrolysis in nitrogen atmosphere, *Fuel Processin. Technol.*, **89**, 21–27.

Ceylan, S., and Topcu, Y. (2014). Pyrolysis kinetics of hazelnut husk using thermogravimetric analysis, *Bioresour. Technol.*, **156**, 182–188.

Demirbas, A. (2004). Effects of temperature and particle size on bio-char yield from pyrolysis of agricultural residues, *J. Anal. Appl. Pyrol.*, **72**, 243–248.

Fantozzi, F., Frassoldati, A., Bartocci, P., Cinti, G., Quagliarini, F., Bidini, G., and Ranzi, E. M. (2016). An experimental and kinetic modeling study of glycerol pyrolysis, *Appl. Energ.*, **184**, 68–76.

Flynn, J. H., and Wall, L. A. (1966). A quick, direct method for the determination of activation energy from thermogravimetric data, *J. Polym. Sci. B Polym. Lett.*, **4**, 323–328.

Garba, M. U. (2013). *Prediction of ash deposition for biomass combustion and coal/biomass co-combustion (PhD thesis*, Leeds University Library), 130–140.

Garba, M. U., Alhassan, M., and Kovo, A. S. (2006). A review of advances and quality assessment of biofuels, *Leonardo J. Sci.*, **9**, 167–178.

Garba, M. U., Umaru, M., Azare, P. E., Kariim Ishaq, U., Onoduku, S., and Mohammad, Y. S. (2016). Characterization and ash chemistry of selected Nigerian coals for solid fuel combustion, *Petroleum and Coal*, **58**, 646–654.

Garba, M. U., Gambo, S. U., Musa, U., Tauheed, K., Alhassan, M., and Adeniyi, O. D. (2017a). Impact of torrefaction on fuel property of tropical biomass feedstocks, *Biofuels*, **9**, 369–377. DOI: 10.1080/17597269.2016.1271629.

Garba, M. U., Inalegwu, A., Musa, U., Aboje, A. A., Kovo, A. S., and Adeniyi, D. O. (2017b). Thermogravimetric characteristic and kinetic of catalytic co-pyrolysis of biomass with low- and high-density polyethylenes, *Biomass Conv. Bioref.*, **8**, 143–150. DOI: 10.1007/s13399-017-0261-y.

Garba, M. U., Ingham, D. B., Ma, L., Degereji, M., Pourkashanian, M., and Williams, A. (2012). Numerical assessment of ash sintering for co-combustion of coal with biomass fuels, *Fuel*, **113**, 863–872.

Garba, M. U., Musa, U., Olugbenga, G., Mohammad, Y. S., Yahaya, M., and Jerome, I. (2018). Catalytic upgrading of pyrolysis oil from bagasse: thermogravimetric analysis and fixed bed pyrolysis, Beni-Suef University, *Journal of Basic and Applied Sciences*. DOI: 10.1016/j.bjbas.2018.11.004

Garba, M. U., Oloruntoba, J. M., Isah, A. G., and Alhassan, M. (2014). Production of solid fuel from rice straw through torrefaction process, *Int. J. Sci. Eng. Invest.*, **4**, 43715–43701.

Haykiri-Acma, H. (2003). Combustion characteristics of different biomass materials, *Energy Conver. Manage.* **44**, 155–162.

Ho, D. P., Ngo, H. H., and Guo, W. (2014). A mini review on renewable sources for biofuel, *Bioresour. Technol.*, **169**, 742–749.

Idris, S. S., Rahman, N. A., and Ismail, K. (2012). Combustion characteristics of Malaysian oil palm biomass, sub-bituminous coal and their respective blends via thermogravimetric analysis (TGA), *Bioresour. Technol.*, **123**, 581–591.

Islam, A., Auta, M., Kabir, G., and Hameed, B. H. (2016). A thermogravimetric analysis of the combustion kinetics of karanja (Pongamia pinnata) fruit hulls char, *Bioresour. Technol.*, **200**, 335–341.

Jekayinfa, S., and Omisakin, O. (2005). The energy potentials of some agricultural wastes as local fuel materials in Nigeria, *Agri. Eng. Int. The CIGR Ejournal.*, **VII**, 1–10.

Katarzyna, S., Pietro, B., and Francesco, F. (2012). Thermogravimetric analysis and kinetic study of poplarwood pyrolysis, *Applied Energy* **97**, 491–497. DOI: 10.1016/j.apenergy.2011.12.056

Kissinger, H. E. (1956). Variation of peak temperature with heating rate in differential thermal analysis, *J. Res. Natl. Bur. Stan.*, **57**, 217.

Li, Z., Zhao, W., Meng, B., Liu, C., Zhu, Q., and Zhao, G. (2008). Kinetic study of corn straw pyrolysis: Comparison of two different three-pseudocomponent models, *Bioresour. Technol.*, **99**, 7616–7622.

Lukas, G., Zuzana, K., and Ľudovit, J. (2009). Kinetic study of wood chips decomposition by TGA, *36th International Conference of Slovak Society of Chemical Engineering.*, May 25–29, 2009, Tatranske Matliare, Slovakia. **178**, 1–14.

Mahir, M. S., Geofrey, R. J., Cuthbert, F. M., and Samwel, V. M. (2014). Analysis of pyrolysis kinetic and energy content of agricultural and Forest waste, *Open J. Renew. Energy Sustain. Develop.*, **1**, 36–44.

Mani, T., Murugan, P., Abedi, J., and Mahinpey, N. (2010). Pyrolysis of wheat straw in a thermogravimetric analyzer: Effect of particle size and heating rate on devolatilization and estimation of global kinetics, *Chem. Eng. Res. Des.*, **88**, 952–958.

McKendry, P. (2002). Energy production from biomass (part 1): Overview of biomass, *Bioresour. Technol.*, **83**, 37–46.

Munir, S., Daood, S. S., Nimmo, W., Cunliffe, A. M., and Gibbs, B. M. (2009). Thermal analysis and devolatilization kinetics of cotton stalk, sugar cane bagasse and shea meal under nitrogen and air atmospheres, *Bioresour. Technol.*, **100**, 1413–1418.

Musa, U., and Aberuagba, F. (2012). Characteristics of a typical Nigerian *Jatropha curcas* oil for biodiesel production, *Res. J. Chem. Sci.*, **2**, 7–12.

Musa, U., Aboje, A. A., Mohammed, I. A., Aliyu, M. A., Sadiq, M. M., and Olaibi, O. A. (2014a). The effect of process variables on the transesterification of refined cottonseed oil, *Proceedings of the World Congress on Engineering 2014 Vol I, (WCE 2014)*, July 2–4, 2014, London, UK, 622–624.

Musa, U., Aboje, A. A., Mohammed, I. A., Aliyu, M. A., Sadiq, M. M., and Olaibi, O. A. (2015). Process optimization, empirical modeling and characterization of biodiesel from cottonseed oil, In Yang, Gi-Chul, Ao, Sio-Long, Gelman, Len (Eds.) *Transactions on Engineering. Technologies*. Springer Science, London, UK.

Musa, U., Mohammed, I. A., Sadiq, M. M., Aliyu, A. M., Suleiman, B., and Segun, T. (2014b). Production and characterization of biodiesel from Nigerian mango seed oil, *Proceedings of the World Congress on Engineering 2014 Vol I, (WCE 2014)*, July 2–4, 2014, London, UK, 645–649.

Nassar, M. M., Ashour, E. A., and Wahid, S. S. (1996). Thermal characteristics of bagasse, *J. Appl. Polym. Sci.*, **61**, 885–890.

Nithitorn, K. B., Witchaya, P., and Suthum, P. (2015). Thermogravimetric Kinetic Analysis of the Pyrolysis of Rice Straw, 2015 International Conference on Alternative Energy in Developing Countries and Emerging Economies, *Energy Procedia*, **79**, 663–670.

Niu, Y., Tan, H., Liu, Y., Wang, X., and Xu, T. (2013). The effect of particle size and heating rate on pyrolysis of waste capsicum stalks biomass, *Energy Sources, Part A: Recovery Utilization, and Environ. Effects*, **35**, 1663–1669.

Nyakuma, B. B. (2016). Pyrolysis kinetics of Melon (Citrullus colocynthis L.) seed husk. https://arxiv.org/pdf/1506.05419

Ogbe, A. O., and George, G. A. L. (2012). Nutritional and anti-nutrient composition of melon husks: Potential as feed ingredient in poultry diet, *Res. J. Chem. Sci.*, **2**, 35–39.

Ounas, A., Aboulkas, A., El Harfi, K., Bacaoui, A., and Yaacoubi, A. (2011). Pyrolysis of olive residue and sugar cane bagasse: Nonisothermal thermogravimetric kinetic analysis, *Bioresour. Technol.*, **102**, 11234–11238.

Ozawa, T. A. (1965). New method of analyzing thermogravimetric data, *BCSJ*, **38**, 1881–1886.

Sachin, K., Ankit, A., and Singh, R. K. (2011). Thermogravimetric analysis of groundnut cake, *IJCEA*, **2**, 268–271.

Senneca, O. (2007). Kinetics of pyrolysis, combustion and gasification of three biomass fuels, *Fuel Process. Technol.*, **88**, 87–97.

Shen, D. K., Gu, S., Luo, K. H., Bridgwater, A. V., and Fang, M. X. (2009). Kinetic study on thermal decomposition of woods in oxidative environment, *Fuel*, **88**, 1024–1030.

Sokoto, M. A., Rawel, S., Bhavya, B. K., Jitendra, K., and Thallada, B. (2016). Non-isothermal kinetic study of de-oiled seeds cake of African star apple (Chrosophyllum albidum) using thermogravimetry, *Physical Chemistry, Analytical Chemistry*, **2**(10). DOI: 10.1016/j.heliyon.2016.e00172.

Sun, W.-G., Zhao, H., Yan, H.-X., Sun, B.-B., Dong, S.-S., Zhang, C.-W., and Qin, S. (2012). The pyrolysis characteristics and kinetics of Jerusalem artichoke stalk using thermogravimetric analysis, *Energy Sources, Part A Recovery, Utilization Environ. Effects*, **34**, 626–635. DOI: 10.1080/15567036.2011.615006.

Slopiecka, K., Bartocci, P., and Fantozzi, F. (2012). Thermogravimetric analysis and kinetic study of poplar wood pyrolysis, *Appl. Energy*, **97**, 491–497.

Vanita, R. M., William, O. S., Ray, L. F., and Payam, M. (2011). Thermal decomposition of bagasse: Effect of different sugar cane cultivars, *Ind. Eng. Chem. Res.*, **50**, 791–798.

Wang, J., Kayoko, M., and Takayuki, T. (2001). High-Temperature Interactions between Coal Char and Mixtures of Calcium Oxide, Quartz, and Kaolinite, *Energy Fuels*, **15**(5), 1145–1152.

Zhou, Z., Hu, X., You, Z., Wang, Z., Zhou, J., and Cen, K. (2013). Oxy-fuel combustion characteristics and kinetic parameters of lignite coal from thermo-gravimetric data, *Thermochim. Acta*, **553**, 54–59.

Zhang, X., Lei, H., Zhu, L., Zhu, X., Qian, M., Yadavalli, G., Wu, J., and Chen, S. (2016). Thermal behavior and kinetic study for catalytic copyrolysis of biomass with plastics, *Bioresour. Technol.*, **220**, 233–238. DOI: 10.1016/j.biortech.2016.08.068

Zhang, X., Xu, M., Sun, R., and Sun, L. (2006). Study on biomass pyrolysis kinetics, *Trans. ASME J. Eng. Gas Turbines Power*, **128**, 493–496.

Nomenclature

α	Degree of conversion
β	Heating rate (K min^{-1})
A	Pre-exponential factor (s^{-1})
E	Activation energy (kJ mol^{-1})
$f(\alpha)$	Conversion function depending on the reaction
$d\alpha/dt$	Conversion rate as a function of time (min^{-1})
$d\alpha/dT$	Conversion rate as a function of temperature (K^{-1})
k	Reaction rate constant (s^{-1})
K	Kissinger
KAS	Kissinger–Akahira–Sunose
$k(T)$	Temperature-dependent rate constant
MSS	Melon seed shell
N	Order of reaction
R	Gas constant (J K^{-1} mol^{-1})
R2	Correlation coefficient
T	Time (S)
T	Absolute temperature (K)
T_0	Starting temperature (K)
T_m	Peak temperature from DTG curve (K)
W_i	Initial weight (wt.%)
W_f	Final weight (wt.%)